Monazomycin-induced Single Channels

I. Characterization of the Elementary Conductance Events

OLAF S. ANDERSEN and ROBERT U. MULLER

From the Department of Physiology and Biophysics, Cornell University Medical College, New York 10021; and the Department of Physiology, Downstate Medical Center, State University of New York, Brooklyn, New York 11203

ABSTRACT Monazomycin (a positively charged, polyene-like antibiotic) induces voltage-dependent conductance changes in lipid bilayer membranes when added to one of the bathing solutions. These conductance changes have generally been attributed to the existence of channels spanning the membrane. In this article we characterize the behavior of the individual conductance events observed when adding small amounts of monazomycin to one side of a lipid bilayer. We find that there are several apparent channel types with one or sometimes two amplitudes predominating. We find further that these fairly similar amplitudes represent two different states of the same fundamental channel entity, presumed to be *the* monazomycin channel. The current-voltage characteristics of these channels are weakly hyperbolic functions of applied potential. The average lifetimes are essentially voltage independent (between 50 and 400 mV). The average channel intervals, on the other hand, can be strongly voltage dependent, and we can show that the time-averaged conductance of a membrane is proportional to the average channel frequency.

INTRODUCTION

It is generally agreed that the voltage-dependent conductance that monazomycin confers upon lipid bilayer membranes is based on the existence of "channels" or "pores." The properties of the macroscopic conductance (Muller and Finkelstein, 1972*a*, *b*) and the observation of excess current noise (Moore and Neher, 1976; Wanke and Prestipino, 1976; Kolb, 1979) are consistent with the idea that monazomycin creates metastable, hydrophilic paths connecting the two aqueous solutions that bathe the film.

Two additional criteria must, however, be met to demonstrate convincingly that the monazomycin-induced conductance is channel mediated. First, it is necessary to resolve at least one type of discrete conductance change in monazomycin-doped bilayers. The occurrence of discrete current jumps at

Address reprint requests to Dr. Robert Muller, Dept. of Physiology, Downstate Medical Center, 450 Clark Ave., Brooklyn, NY 11203.

J. GEN. PHYSIOL. © The Rockefeller University Press · 0022-1295/82/09/0403/24 $1.00 403
Volume 80 September 1982 403–426

constant membrane potential is usually taken as a reflection of state changes in individual molecules or well-defined molecular aggregates. Although unitary conductance changes need not be rectangular in shape, all known examples have state transitions so fast (compared with the limiting time constant of the recording apparatus) as to appear instantaneous. In fact, we may go so far as to say that it is the existence of large enough rectangular current pulses that makes us comfortable with describing a conductance as channel mediated.

This first criterion was met some time ago for monazomycin-modified bilayers (Muller and Andersen, 1975; Bamberg and Janko, 1976). In this paper our aim is to further characterize the functional properties of monazomycin channels. Our major conclusions are easily stated. First, there are several distinguishable current amplitudes for jumps between the "open" and "closed" states, with one or sometimes two amplitudes predominating. Second, the current-voltage characteristic of single channels is a weak hyperbolic sine function of the membrane potential (V), such that the channels are ohmic for $V < 100$ mV. Third, the average channel lifetime is essentially invariant to changes of V. Finally, there is a direct proportionality between the time-averaged conductance of a bilayer and the frequency of channel openings.

The second criterion for demonstrating the channel basis of a conductance seems obvious: it must be shown that various properties of the macroscopic conductance can be accounted for when suitable averages are taken for the corresponding single-channel properties. Perhaps more correctly, because the macroscopic conductance (G) is generally better characterized, it is necessary to find critical features of the single channel that are predicted from G. For example, if the macroscopic conductance has known ionic selectivities, it should be possible to predict the zero-current potential of individual channels. This connection was made for gramicidin A by Eisenman et al. (1976). Similarly, if a conductance is chemically controlled, a proof of mechanism would require the channels to show the expected sensitivity to pharmacological agents. This was achieved for the acetylcholine-activated conductance of vertebrate neuromuscular junctions by Neher and Sakmann (1976).

For a voltage-dependent conductance such as monazomycin, the second criterion is best satisfied by looking for an aspect of the channel statistics that varies in the "correct" way with membrane potential, as was done for the excitability-inducing material channel by Ehrenstein et al. (1970). Given that the only properties that can vary for channels are their amplitude, lifetime, and frequency of occurrence, and given that for monazomycin two of these are insensitive to voltage, it would seem that frequency is, *reductio ad absurdum*, the relevant variable. Indeed, because of the direct proportionality between frequency and time-averaged conductance, the answer seems straightforward. Nevertheless, the connection was very difficult to make, because the channel frequency often did not vary with voltage in the same exponential fashion that the macroscopic conductance did.

We believe we have resolved this problem in a satisfactory way. In the article that follows (Muller and Andersen, 1982), we show that there are circumstances in which the occasional loss (or even reversal) of the voltage dependence of channel frequency is to be expected. Our ability to explain the

complex relationship between channel frequency and membrane potential in the face of the much simpler relationship that exists between macroscopic conductance and voltage is based on a continuous model that accurately describes the kinetics of the macroscopic conductance (Muller et al., 1981; Muller and Peskin, 1981).

For completeness, it would be nice to have a stochastic model that yields the continuous model in the limit of very high channel frequency. Nevertheless, the continuous model allows for a complicated frequency-voltage characteristic and predicts several other interesting peculiarities of channel behavior. Because we have been able to observe these peculiarities experimentally (Muller and Andersen, 1982), we conclude that channel frequency variations are the basis of the voltage dependence of the macroscopic monazomycin conductance.

MATERIALS AND METHODS

Membrane-forming Solutions

Two separate series of voltage-clamp experiments were carried out. The first (which we will not deal with in detail) was done with phosphatidylethanolamine/*n*-decane (2.5% wt/vol; PE) as the membrane-forming solution. These membranes (0.12 mm^2) were made by the brush technique of Mueller et al. (1963) in symmetrical, unbuffered NaCl solutions ([NaCl] $\geq$ 4.0 M) at room temperature. The second, major set used phosphatidylglycerol/cholesterol/*n*-decane (1%/1% wt/vol; PGC) as the membrane-forming solution. The membranes (1.6 mm^2) were formed at 25°C by the pipette technique of Szabo et al. (1969) in symmetrical, unbuffered 0.1 M NaCl solutions. We were able to use the same ionic strength in these experiments as was used for work on the macroscopic conductance because of the high negative surface charge density of PGC films ($\sim 2 \times 10^{14}$ charges$\cdot cm^{-2}$). With uni-univalent salts, the nominal surface concentration of the cation is high enough ($\sim$10 M) to ensure that the single-channel currents can be resolved.

The single-channel recordings in this main series were done with a micropipette technique, which is described in detail elsewhere; we will only give a summary here. A fire-polished, silanized glass pipette is mounted in a microelectrode holder. The pipette tip is first coated with the membrane solution by pushing it into and out of the torus of the large film. The tip is then advanced up to and through the original plane of the large film so that a local bulge is produced (Fig. 1A1–2). Electrically, we can detect this partial occlusion of the pipette by a noise reduction of ~60% (Fig. 1B1–2). For PGC films in 0.1 M salt, the small membrane "seals" onto the tip after a waiting time of 0.5–5 min (Fig. 1A2–3). *Pari passu*, the noise recorded by the current-to-voltage converter drops dramatically (Fig. 1B2–3) to reach a value comparable to the Johnson noise of the feedback resistor.

We believe that the waiting time for sealing is caused by the mutual repulsion of the double layers of the membrane and the silanized glass, which arise from negative fixed charges on the two surfaces. In line with this are the observations that the waiting time is reduced to nearly zero for PGC films in 1.0 M salt and is nearly zero, independent of salt concentration, for the much less charged PE films (see also Andersen, 1982).

Electrical Measurements

We used a standard two-electrode voltage clamp; contact to the bathing solutions was made via Ag/AgCl electrodes. The output from the current-to-voltage converter

was amplified (× 10 to × 1,000) and then fed to two separate low-pass filters (model 4211 or 4213; Ithaco, Ithaca, NY; or model 3322 R; Kronheit, Avon, MA). The cutoff of one filter was set between 0.01 and 0.1 Hz; the output went to the "slow" channel of a stripchart recorder (Brush model 220; Gould, Cleveland, OH). The output of the other filter, whose cutoff was set between 10 and 160 Hz, went to the other, "fast" channel of the stripchart recorder. We also observed the "fast" signal on a storage oscilloscope.

The fast recording was used to visualize the membrane channel activity. For the earlier (PE) experiments, we generally had the low-pass filter set between 10 and 40 Hz. The cutoff range was raised to 50 to 100 Hz for the PGC experiments; this was

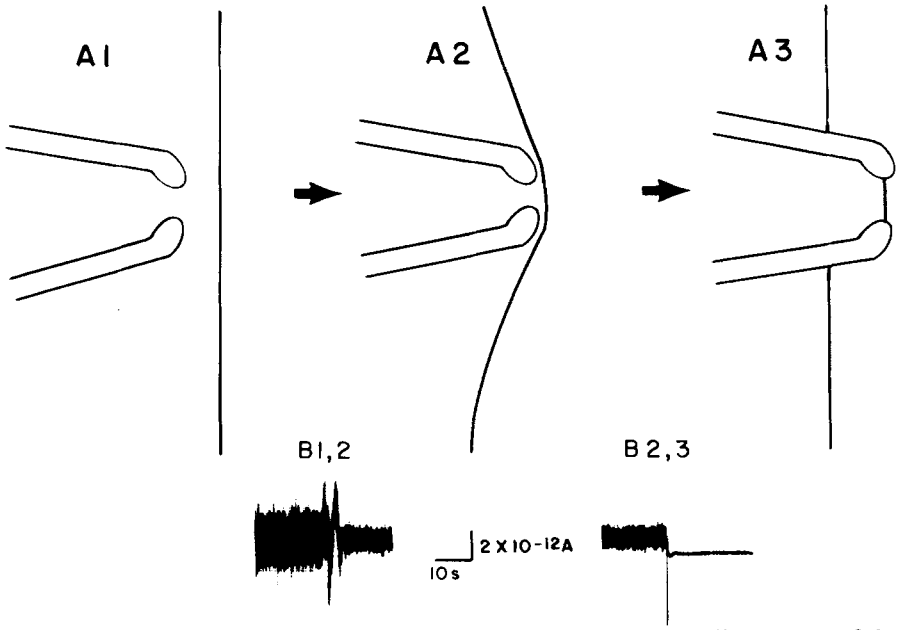

FIGURE 1. Formation of a small membrane. Top: schematic illustration of the membrane events. Bottom: the changes in current noise observed concommittantly with the state transitions shown in the upper half. Note that the mere occlusion of the pipette by the large membrane (A2) causes an ~60% decrease in the current noise (B1, 2). The fusion of the small bilayer with the pipette (A3) causes a further ~90% drop of the noise (B2, 3).

possible because of the great noise reduction afforded by the micropipette technique. The slow recording was used to get a direct indication of the time-averaged current (and therefore the conductance). In other words, we used the 0.01–0.1-Hz filter as a leaky integrator. Values of the conductance read from this record will be symbolized by "*G*." Unitary conductances, obtained from the step size of a rectangular current-pulse, will be symbolized by "*g*." To minimize input noise to the voltage clamp, the chamber was put inside a rigid Faraday cage, which in turn was mounted on an air-suspension table (Servabench Mark IV; Barry Systems, Watertown, MA).

We make our electrical sign convention with respect to the asymmetrical monazomycin concentration. The virtual ground of the voltage clamp was connected to the

monazomycin-free (*trans*) solution, so that potential differences are equal to the potential of the *cis* solution. Positive current is defined to flow from *cis* to *trans*. By way of orientation, more positive potentials are associated with higher *G*.

Initial Stimulation Protocol

After the membranes were visually black, a small aliquot of a stock solution of monazomycin in water (2.0–20.0 μg/ml) was added to the *cis* solution to achieve a final concentration between 4 and 20 ng/ml. Electrical measurements were not attempted until ~5 min after addition of monazomycin.

In general, we found it impossible to step the potential to a fixed value and merely wait until channel activity of a useful intensity appeared (see also Muller and Andersen, 1982). Just applying a potential which from past experimental experience was associated with reasonable channel frequency (i.e., a low probability for two or more channels) would not cause the fast recording to budge from its baseline. Instead, it was necessary to set the voltage to a very high positive level (up to 600 mV, depending on the monazomycin concentration) to initiate activity. Shortly after applying the very high potential, single channels were easily resolved, but their frequency rapidly grew to levels far too high for useful measurements. Accordingly, the potential was reduced until activity decreased to a level at which it was possible to see the unitary events. This hysteresis is just the first example of how difficult it is to get to a true steady state when very few monazomycin channels are opening. In the next paper we will describe this phenomenon (and others like it) in more detail.

Measurements of Channel Properties

All measurements of the amplitudes and durations of channels and of the intervals between channel openings were done by hand from the original pen-writer records. The amplitude of a channel-like event was included in our samples if it met the following criteria. First, it had to have an obvious plateau. In practice, this meant that its duration had to exceed ~20 ms due to the limited high-frequency response of the pen-writer and/or the high-frequency cutoff of the filter. Second, we measured amplitudes only if the channel arose directly from the baseline noise and returned to it directly; we did not include amplitudes of events that appeared as two or more simultaneously conducting channels. An exception to this criterion was made for what we will refer to as Δ or compound channels (see Results). This was done after we were led to conclude that the channels exemplified in Fig. 4 were not small channels randomly occurring on top of large ones. Finally, we rejected events for which the baseline noise (for whatever reason) differed by >0.8 mm (the size of the finest-ruled division on the pen-writer paper) just before and just after the event. Only channels whose amplitude was deemed acceptable for analysis were included in our lifetime samples. A consequence of this decision is that the number of short-lived channels often appeared to be too small for a first-order death process.

With regard to analyses of intervals between channels, we used much simpler standards. In this case, an event was considered to be a channel if its jump was greater than about three times the thickness of the baseline noise. An interval was defined by the time between successive upward jumps, regardless of their amplitudes.

Reagents

Monazomycin was a gift from Drs. Yonehara and Ōtake of the University of Tokyo. Cholesterol was bought from Eastman Kodak Co. (Rochester, NY) and recrystallized twice from ethanol. PE and PG were obtained from Supelco (Bellefonte, PA). The PE

was used without further purification. The PG was put into the acid form with 0.01 M H_2SO_4 and extracted into ethyl ether. It was then dried and re-dissolved in chloroform/methanol (2/1; vol/vol). *n*-Decane was purchased from E. Merck (via EM Laboratories; Elmsford, NY), Analabs (North Haven, CT), or Chemical Samples Co. (Columbus, OH). NaCl was either AR grade (Fisher Scientific, Pittsburgh, PA) or Suprapur grade (E. Merck via MCB Inc., Cincinnati, OH). We used de-ionized water from a Milli-Q system (Millipore Corp., Bedford, MA).

RESULTS

The Form of Individual Monazomycin Channels

We find that the monazomycin-induced conductance is based upon the existence of perhaps five channel populations that are distinguishable on the basis of their amplitudes. Fig. 2 is an amplitude histogram based on 1,257 channels recorded during an extended run (20 min) at an applied potential of 200 mV. The five populations are, for the moment, defined by the existence of five modes. The mean conductance for each channel type is given Table I. Fig. 3 shows examples of each type of channel, taken from the original pen-writer record.

From the amplitude histogram of Fig. 2 and the fact that there are no striking differences in the mean lifetimes of the several channel types, it is apparent that, at least near 200 mV, almost all of the conductance is caused by the fourth peak ($I = 1.03 \times 10^{-12}$ A; i.e., $g = 5 \times 10^{-12}\ \Omega^{-1}$). Although the existence of peaks 1–3 may ultimately tell us a great deal about the molecular basis of the conductance (assuming they are not caused by contaminants or compounds similar to monazomycin), we feel they may safely be ignored as we try to account for the time-averaged conductance through a monazomycin-modified membrane. By contrast, as we will show below, the channels in peak 5 are closely related to those in the major peak. The properties of the channels in these two peaks will therefore be considered in some detail.

Closer inspection of our pen-writer tapes reveals the presence of a considerable number of events such as those shown in Fig. 4. Although these might be interpreted as being caused by the opening of a peak-1 channel on top of a peak-4 channel, several arguments lend credence to the idea that they are single channels with two rather similar open states.

The total duration of the run at 200 mV was 1,200 s. Of this time, the current was in the range of peak 4 for 59.4 s.[1] The time the current was in the peak-1 range totaled 1.7 s, whereas that spent in the higher conductance state of a composite channel was ~8 s. The conditional probability of a small jump during a peak-4 channel is thus ~90 times greater than a small jump from the baseline.

We can reinforce the impression gained from this calculation by referring to the oscillograms of Figs. 5A and B. Fig. 5A is a multisweep record taken at

[1] This includes only the time for channels well defined enough to allow amplitude and duration measurements. In practice, a channel had to remain open for at least 20 ms for a clear-cut level to be seen. Nevertheless, even if we double the 59.4 s, a ridiculous overestimate, our conclusions are unchanged.

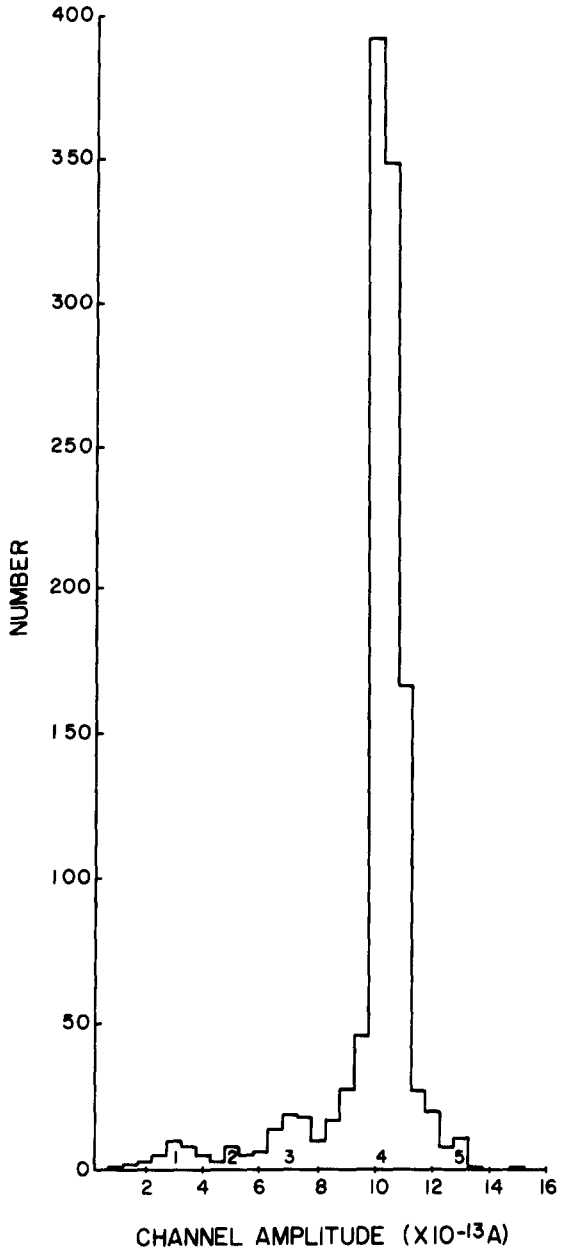

FIGURE 2. Histogram of the current jump amplitudes seen at 200 mV. Only channels arising and returning directly to the baseline were measured; moreover, Δ channels (see Fig. 4 and *Form of Individual Monazomycin Channels* in Results) were not included in the histogram. The five channel populations discussed in the text are defined by the existence of the five modes shown. The means given in Table I were calculated using the modal bin and the two adjacent bins for all peaks save number 4, where we used the modal bin and the two adjacent ones on either side.

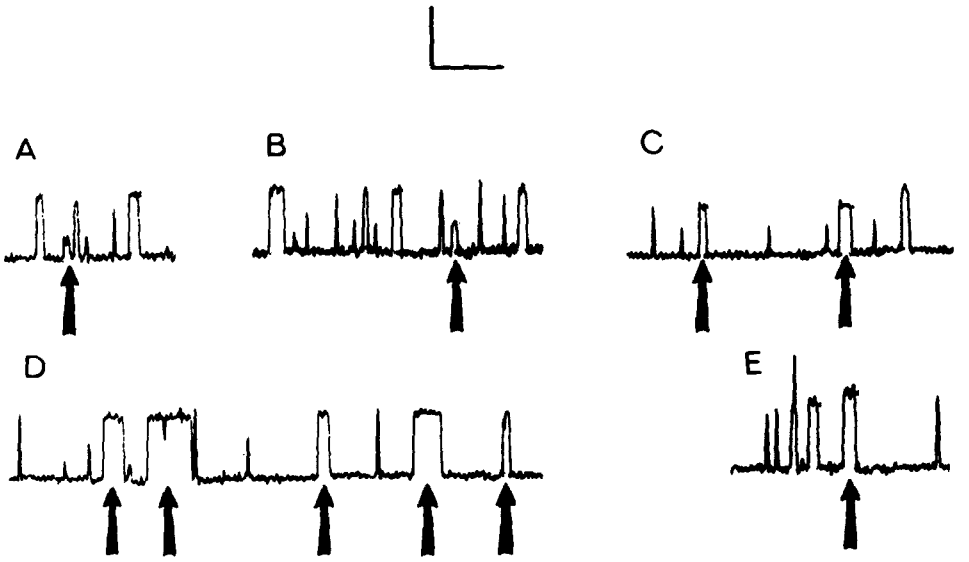

FIGURE 3. Examples of current-jump events from each mode of Fig. 2. A–E show, respectively, channels from peaks 1–5. The relevant events are marked by arrows; the high-probability peak-4 channels seen in each record serve as convenient references for comparison. Vertical calibration mark = 10^{-12} A. Horizontal calibration mark = 0.4 s.

TABLE I
MEAN CONDUCTANCES OF THE FIVE CHANNEL MODES OF FIG. 2*

Mode	Mean channel conductance (Ω^{-1})
1	1.5×10^{-12}
2	2.5×10^{-12}
3	3.5×10^{-12}
4	5.1×10^{-12}
5	6.4×10^{-12}

* The applied membrane potential was 200 mV.

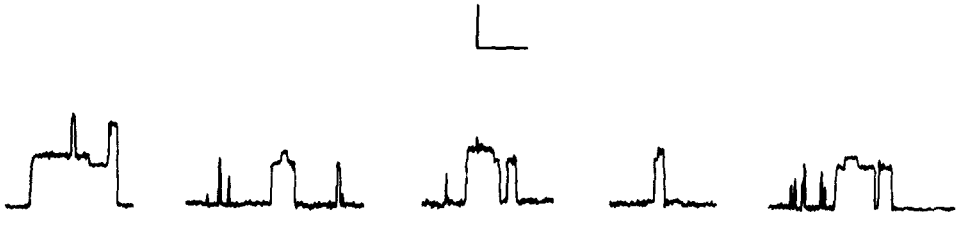

FIGURE 4. Examples of composite or Δ channels taken from the same record as was used for the histogram of Fig. 2 and for the examples of Fig. 3. Vertical calibration mark = 10^{-12} A. Horizontal calibration mark = 0.4 s.

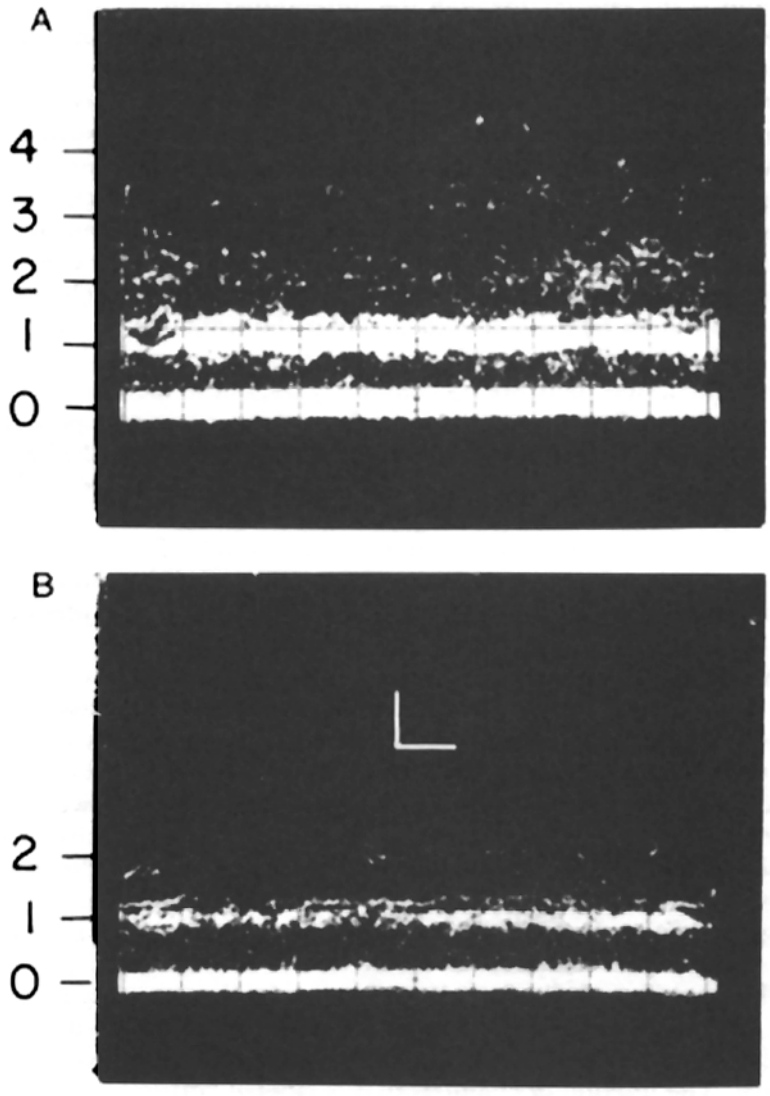

FIGURE 5. Superimposed oscilloscope sweeps of the fast current record. Top: the presence of several well-defined current levels is evident in the upper picture; the numbers at the left indicate the number of conducting channels associated with each level. Note that the one-channel level is noisier than the ground level (no channels). The number of superimposed sweeps is ~200. Bottom: a multi-sweep record taken immediately after the one shown at the top. Many fewer sweeps were used here (~20) to show the splitting of the one-channel band into two sublevels. The difference between these levels is equal to the size of the Δ jumps. Vertical calibration mark = 10^{-12} A. Horizontal calibration mark = 0.1 s. The applied potential was 200 mV.

200 mV just before the 1,200-s pen-writer run, using a storage scope. The lowest band is the current through the unmodified film, whereas the upper bands represent the currents that flow while one, two, three, and (with some imagination) four channels from peak 4 are conducting. The fact that the one-channel band is thicker than that for the ground state does not indicate that more time was spent with one than with no conducting channels. Rather, the increased thickness of the one-channel band arises because the current associated with this band fluctuates more than the current associated with the ground-state band. This is illustrated in Fig. 5B, where we can see that the one-channel level of Fig. 5A is composed of two quite similar current levels. The difference between the "noisy" one-channel band and the "clean" ground-state band provides additional evidence that the small (or Δ) transitions are features primarily associated with peak-4 channels.

It seems, then, that there are six channel types, but in fact we can show that peaks 4 and 5 and the compound channels really comprise one population. In the first place, we note the similarity of the average step size (2.37×10^{-13} A) and the difference of the mean currents of peaks 5 and 4 (2.53×10^{-13} A); this obtains despite the small sample in peak 5.

The situation is more obvious at other potentials. Fig. 6 (bottom) is a histogram of "simple" channel amplitudes at 100 mV. Of the four modes, the upper three correspond to peaks 3, 4, and 5 of Fig. 3; the identity of the meager sample at low amplitudes is problematical. Fig. 6 (top) is a histogram of the Δ steps we found arising from channels in peak 4. We have set this histogram so that the zero bin (no step) is directly above the mean for peak 4, with the result that current levels for peak 5 and the Δ peak virtually coincide.

That these three channel "types" represent three different manifestations of the fundamental monazomycin-induced conductance events will be further supported by an analysis of channel lifetimes and of the transitions between states (see *Channel Lifetimes*). We will therefore use the term "monazomycin channels" to refer to these three channel states collectively.

In Fig. 7, we plot the probability of occurrence of the three manifestations of the monazomycin channels as a function of voltage. Also plotted is the summed probability of all other channel types. With increasing potential, the fraction of channels in peak 4 increases, whereas that in peak 5 decreases. The probability of two-state channels reaches a (statistically significant) maximum at 100 mV. The fraction of channels that is labeled "other" is at most 18% of the population (at 50 mV). Although it may seem surprising to the reader, as it did to us, that the upper level of monazomycin channels is destabilized with increasing potential, in reality our knowledge of the actual molecular events that underlie this conductance is so scant as to be neither affirmed nor denied by this observation. (If we assume a "barrel-stave" structure for the channels, then an interpretation of the steps would be that one more [positively charged] monomer had beeen added, thus increasing the lumenal diameter of the channel. In this view, it would seem "natural" for the peak-5 probability to increase with positive potential increases.)

In summary, we believe that the monazomycin conductance is largely based

on the existence of a single-channel type that has two open states whose current levels differ by ~30%. An individual event may go from the ground state (no channel) to the peak-4 or to the peak-5 level and then return to the ground state, or it may switch between the two levels before ending.

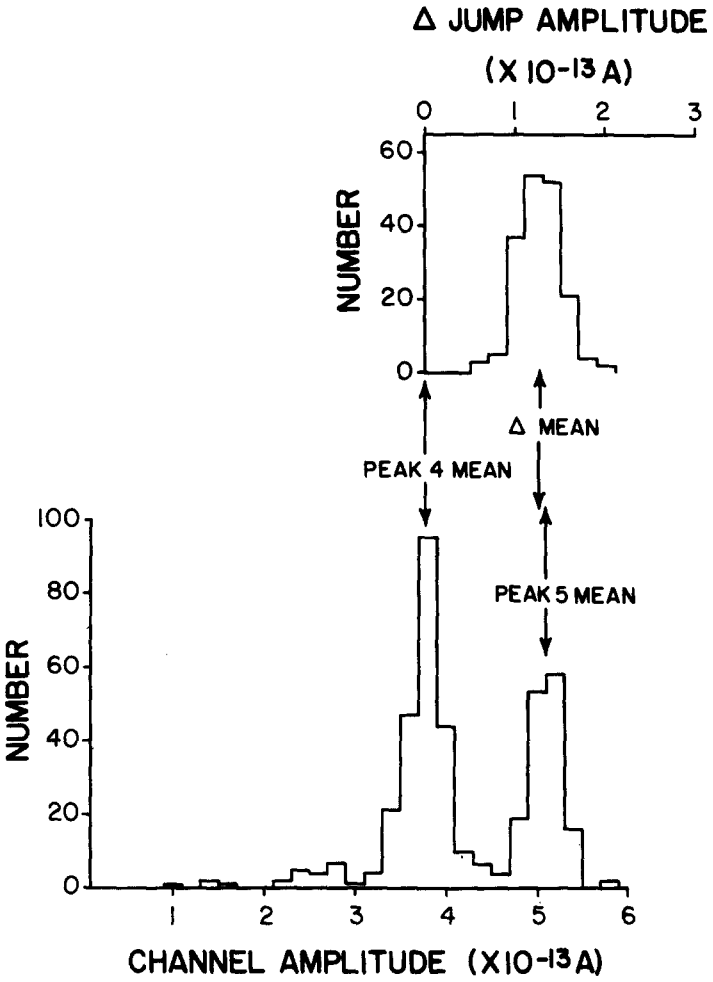

FIGURE 6. Histogram of current-jump amplitudes at $V = 100$ mV. Bottom: note the two well-defined peaks at $I = 3.75 \times 10^{-13}$ A and $I = 5.1 \times 10^{-13}$ A. There is also a diffuse scattering of channels at lower currents. The sample size for the main histogram is 403. Again, only channels arising from and returning directly to the baseline were analyzed. All Δ channel (see Fig. 4) amplitudes are plotted in the upper histogram. Top: histogram of the Δ jump amplitudes; the plotted amplitude is the current change associated with a transition from an open peak-4 channel to the peak-5 level. The histogram is set with its zero (no Δ jump) amplitude directly above the mean for the peak-4 ($I = 3.75 \times 10^{-13}$ A) channels, with the result that the mean jump nearly coincides with the mean of the peak-5 (5.1×10^{-13} A) channels.

Current-Voltage Properties of Monazomycin Channels

In agreement with measurements made on high-conductance (i.e., many-channel) monazomycin-modified films (Muller and Finkelstein, 1972*a*), we find that the current-voltage characteristic of single channels in symmetrical salt is ohmic up to ~150 mV. At higher potentials, the i–V curve becomes supralinear. In Fig. 8, we present a set of i–V points for the peak-4 state over the range $50 \leq V \leq 400$ mV.

The experimental points are well fitted over the whole range of V by:

$$i = g_o \frac{2kT}{Bq} \sinh\left(\frac{BqV}{2kT}\right) \tag{1}$$

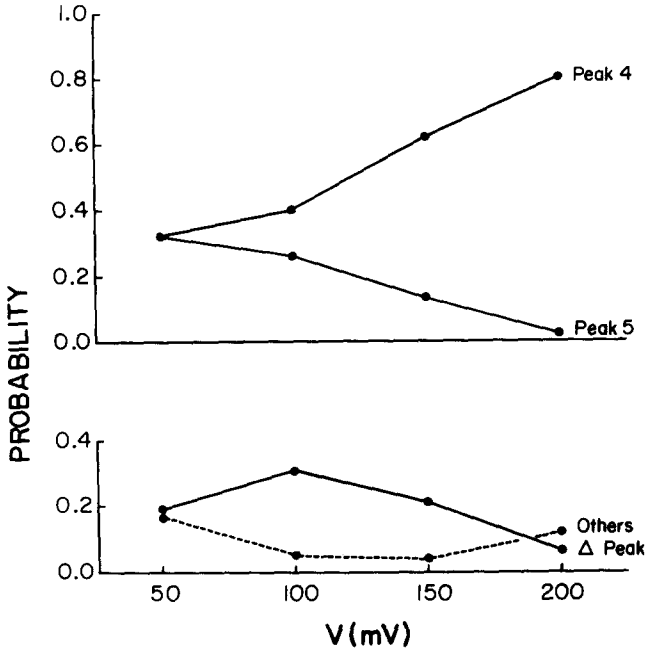

FIGURE 7. Probability of observing peak-4, peak-5, Δ channels, and all other types combined, as a function of membrane potential. The figure is broken into two parts to ease reading, but the summed probability for all four lines is 1 at any potential.

where g_o is the slope of the i–V curve in the ohmic range (i.e., the small signal conductance) and B is an empirical parameter ($0 \leq B \leq 1$). As usual, q is the electronic charge, k is Boltzmann's constant, and T is the absolute temperature. The best fit is obtained with $B = 0.30$ and $g_o = 4.05 \times 10^{-12}\ \Omega^{-1}$.

Formally, Eq. 1 ascribes the shape of the i–V characteristic to the existence of a single, symmetrical energy barrier to ionic movement for which only a fraction, B, of the applied voltage falls across the barrier (see, for example,

Andersen and Fuchs, 1975). In the present case, however, we do not have enough information to say whether this formal picture is realistic, because the stationary i–V relationship reflects the properties of all energy barriers that the ion must traverse in moving through the channel. In particular, given that we have no idea about where we are operating on the conductance vs. concentration curve, Eq. 1 should be regarded as a purely phenomenological expression.

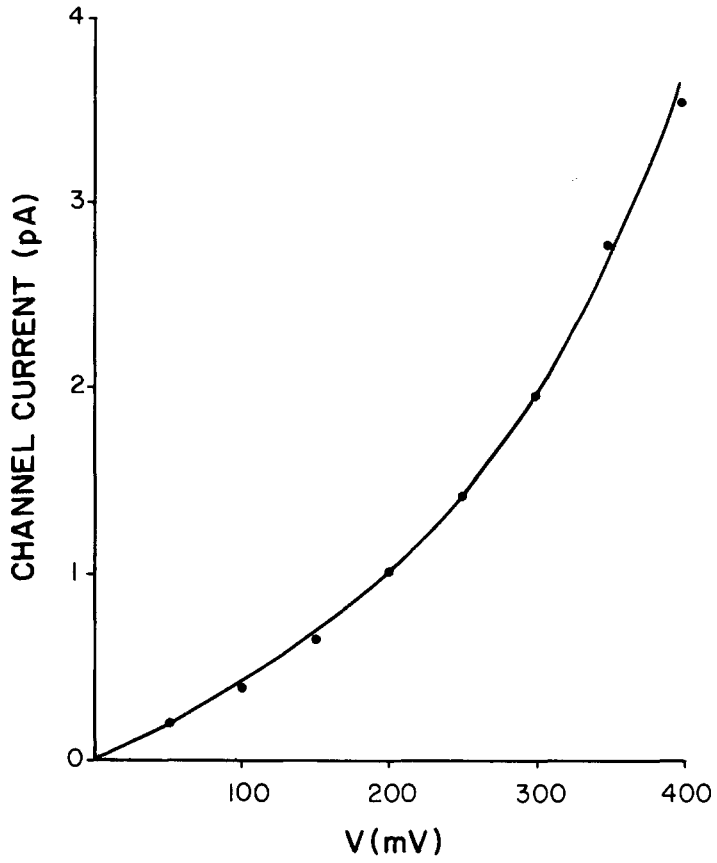

FIGURE 8. Current voltage characteristics of monazomycin channels in the peak-4 state. The points denote the (unweighted) mean currents calculated from the peak-4 mode of the amplitude histogram at each applied voltage. Each point is generally based on several independent experiments. The solid line is calculated according to Eq. 1 with $g_o = 4.05$ pS and $B = 0.30$.

From the form of the i–V characteristic, it is evident that nonlinearity of the current through individual channels resulting from changes in V cannot begin to account for the extraordinary voltage dependence of the monazomycin conductance. To underscore this point, we stress that essentially all of the work on the macroscopic conductance has been done at potentials for

which the channels behave ohmically. It is interesting, in this regard, that the voltage-dependent shift in the most likely state of the channels toward the peak-4 state is in the direction to keep the average conductance ohmic, even as the i–V characteristic begins to become measurably supralinear.

Channel Lifetimes

Let us assume that the monazomycin channels are indeed a single population that subsumes the peak-4, peak-5, and Δ channels. We find for this aggregate that the distribution of channel lifetimes is well described by a single exponential process over a wide voltage range: $N(t) = Ne^{-t/\tau}$ where N is the number of channels in the sample and τ is the average lifetime. t is the time that elapses after a channel opens and $N(t)$ is the number of channels with lifetimes $>t$. A graph of $N(t)$ vs. t is appropriately referred to as a survivor plot (Cox and Lewis, 1966).

In Fig. 9, we show that plots of log $[N(t)/N]$ vs. t for three different voltages all yield fairly good straight lines with similar slopes. The average channel duration, read from the linear portions at short durations, are, respectively, 46, 44, and 41 ms for the 100-, 200-, and 300-mV experiments. A more extensive set of measurements over the voltage range $50 \leq V \leq 400$ mV leads to the following conclusions. First, the range of average lifetimes is fairly narrow (33–52 ms). Second, there is no systematic trend of average lifetime with voltage. Because the average channel duration is (within experimental limits) independent of membrane potential, this factor cannot account for the voltage dependence of the macroscopic conductance.

The nonlinearity at 200 mV (excess number of long-lived channels) is an uncommon feature. Given that the tail represents only 3% of the sample, it is probably just noise. Even if the tail proves to be a real property of the system, it cannot be important quantitatively. By contrast, we feel that the deficit of "counts" in the 0–20-ms bin for the 100-mV sample is probably an artifact of our measurement technique: we do not analyze a channel for amplitude or duration unless it lasts long enough for its level to be unambiguous. This means that we must lose short-lived channels at a higher rate when the applied potential is lower, because we must set the filter cutoff at a lower frequency to compensate for the reduced amplitude of the unitary currents.

Although we have not studied the transitions of a channel (once it opens) between states 4 and 5 in sufficient detail to preclude other, more complex possibilities, we believe that each channel must first go into state 4 and must close from state 4. In this view, a peak-5 channel is simply a Δ channel for which the transitions from state 4 to state 5 and from 5 to 4 occur, respectively, so close to the appearance and disappearance of the channel as to be unresolved.

Two pieces of evidence lend support to our contention. First, the great majority of composite or Δ channels are indeed observed to open to and close from the peak-4 state, as illustrated in the second and fifth examples of Fig. 4. Indeed, we had to make a fairly determined search for Δ channels that apparently opened to state 5 (Fig. 4, first and third examples) or closed from state 5 (Fig. 4, fourth example). Second, we did a Monte Carlo analysis of our

model, choosing Markov transition probabilities for jumps from state 4 to state 5, for closing from state 4 and for jumps to state 5 from state 4. We found that when the probability for closing is much greater than the probability of a jump to state 5, the forms of lifetime histograms for four aspects of

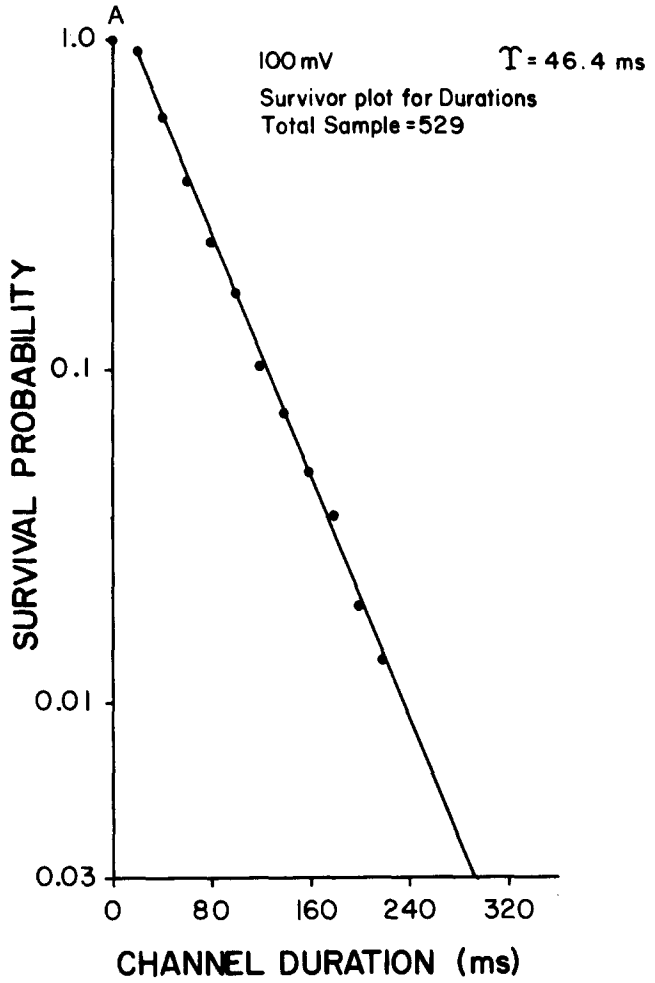

FIGURE 9. Survivor plots of single-channel lifetimes. All peak-4, peak-5, and Δ channels are included in each plot. The ordinate is log $[N(t)/N]$ to facilitate comparisons among the three sets of data. Note the similarity of the slopes at 100, 200, and 300 mV; their near identity is the sole reason we present these data in three separate panels. The bin width for analysis of lifetimes was 20 ms for the 100-mV plot and 40 ms for the 200- and 300-mV plots.

the channels' properties were reproduced. In particular, we were able to see an apparently first-order death process for all channels, an apparently first-order process for the first jump to state 5, and an apparently first-order death process for channels that never entered state 5. The lifetime histogram for

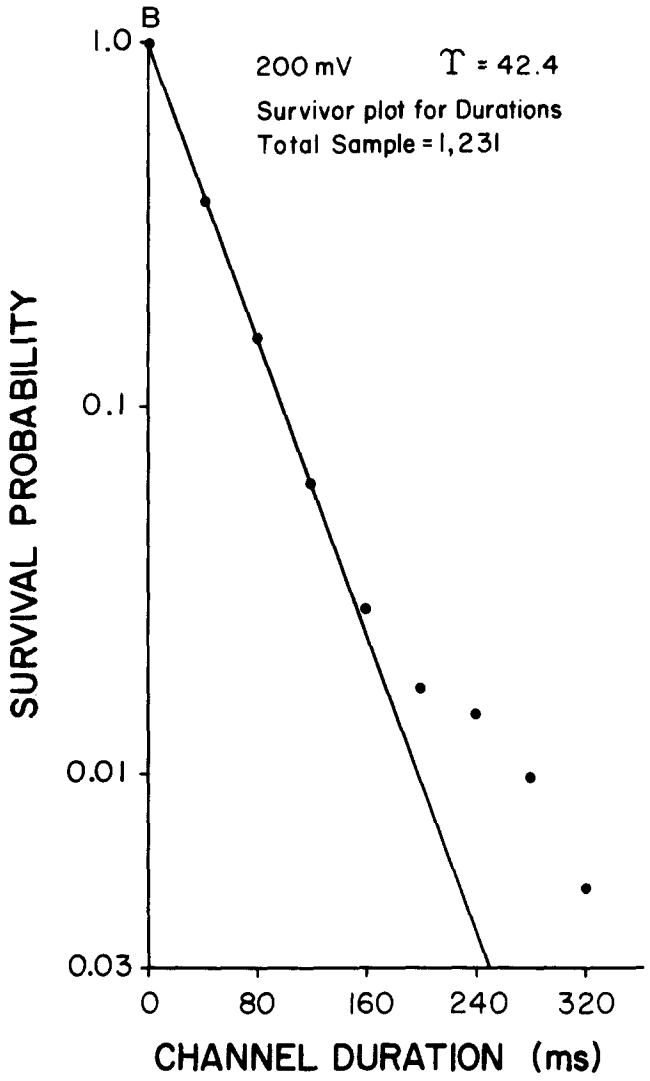

channels that entered state 5 at least once that was generated by the model had its maximum clearly displaced away from the first several 40-ms bins, in accord with our data (not shown).

Channel Frequency

Fig. 10 contains survivor plots for the intervals between channels (i.e., the time span defined by the opening of a channel and the opening of the next channel; in measuring the intervals, we ignored the fact that more than one channel population exists).

Because the plots of log $[N(t)/N]$ vs. t are straight lines, the intervals are exponentially distributed. Although this is not a proof, it is a good indication that the individual channels occur independently of one another. More

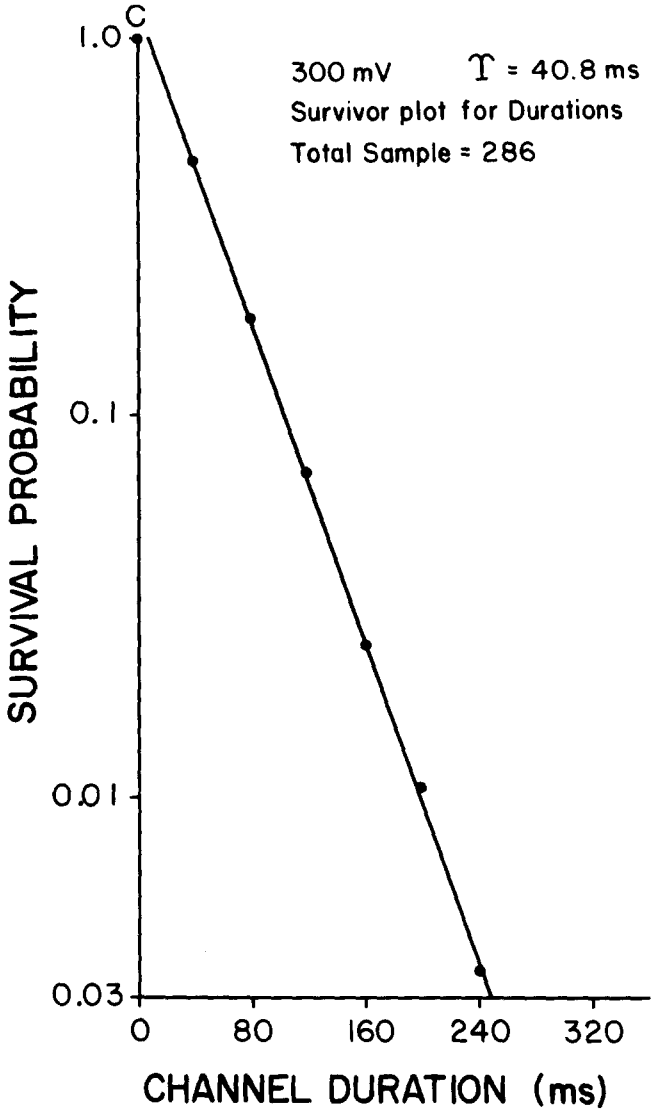

importantly, however, we see that the slopes of the lines vary strongly with potential, although not nearly so strongly as does the macroscopic conductance. The average interval (or its reciprocal, the average channel frequency) is therefore a channel parameter whose variations could be responsible for the macroscopic voltage dependence. In the next paper we will conclude, in a more positive vein, that channel frequency does indeed vary with voltage in the appropriate fashion, but for now we simply assert that the connection is very complex.

The finding that the intervals are exponentially distributed allows us, with no loss of information, to measure channel frequency merely by counting the

number of channel openings per second. In Table II we compare frequencies obtained this way with the reciprocals of the averaged intervals. The close agreement proves that the simpler method is valid.

Fig. 11 contains the major result of this paper, the demonstration that variations in channel frequency account for variations in the monazomycin-

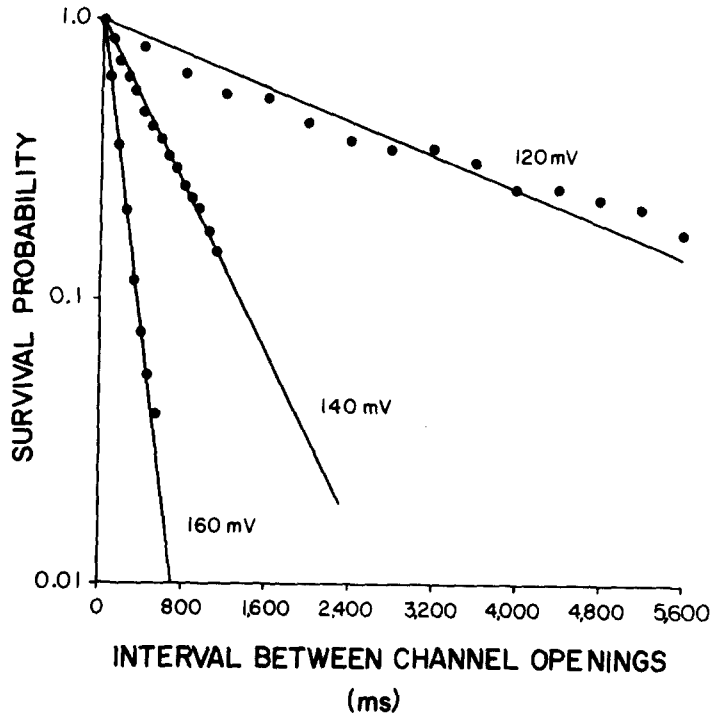

FIGURE 10. Survivor plots for the intervals defined by successive channel openings at 120, 140, and 160 mV. Note that the slopes are very different, despite the relatively narrow range of V. The sample sizes and average channel frequencies were: 52 intervals and 0.35 channels s^{-1} at 120 mV; 271 intervals and 1.6 channels s^{-1} at 140 mV; 334 channels and 6.0 channels s^{-1} at 160 mV. The bin width for intervals was 80 ms at 160 and 140 mV and was 400 ms at 120 mV.

TABLE II

COMPARISON OF TWO METHODS OF ESTIMATING CHANNEL FREQUENCY

V	Opening frequency (s^{-1})*	$1/\tau$ (s^{-1})‡
mV		
120	0.30	0.35
140	1.5	1.6
160	6.2	6.0

* Channel frequency was obtained by counting the number of openings per second.
‡ Channel frequency was calculated from the reciprocal of the time constant of interchannel interval survivor plots (Fig. 10).

induced current (A) and conductance (B). In Fig. 11A we plot slow-channel current (I_s) against channel frequency; I_s is uncorrected for the leakage current through the unmodified membrane. These essentially "raw" data were obtained with the following experimental protocol: V was set to a selected value and left there until I_s reached an apparent steady state. The chart recorder was then run for 1 min at sufficiently high speed (25 mm s^{-1}) to allow individual current jumps to be resolved. An interval of 1 min was then allowed to pass before the next high-speed, analyzable record was taken. We obtained at least two, but generally three, 1-min samples at a given V before changing to a new V. The points in Fig. 11A represent a total of 19 runs at V = 120, 130, 140, 145, 150, 155, and 160 mV; only 17 points are visible because two data-point pairs coincided. The channel frequency was estimated simply by counting the number of openings in 60 s. The slow current for each run was obtained by averaging 30 measurements from the paper tape.

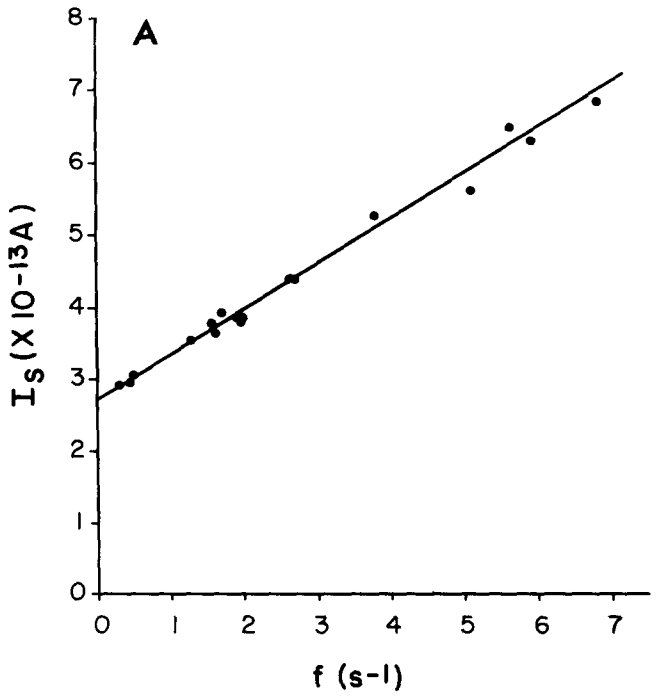

FIGURE 11. A. Plot of average current from the slow channel of the pen-writer; I_s vs. average channel frequency, f. The current intercept for $f = 0$ corresponds to the current through the unmodified bilayer at 120 mV. The data were obtained in the voltage range $120 \leq V \leq 160$ mV. Points from a total of 19 1-min runs were analyzed, but only 17 are visible because two pairs of points were coincident. The line is drawn with a slope of 6.3×10^{-14} C/channel. B. Channel-related conductance vs. average channel frequency, f. The transition between I_s and G_∞ was made as described in the text. The points here are average for all runs at a given V for the membrane used. Going up and to the right from the origin, the voltage for successive points was 120, 130, 140, 145, 150, 155, and 160 mV. The slope of the line is 2.1×10^{-13} Ω^{-1} s/channel.

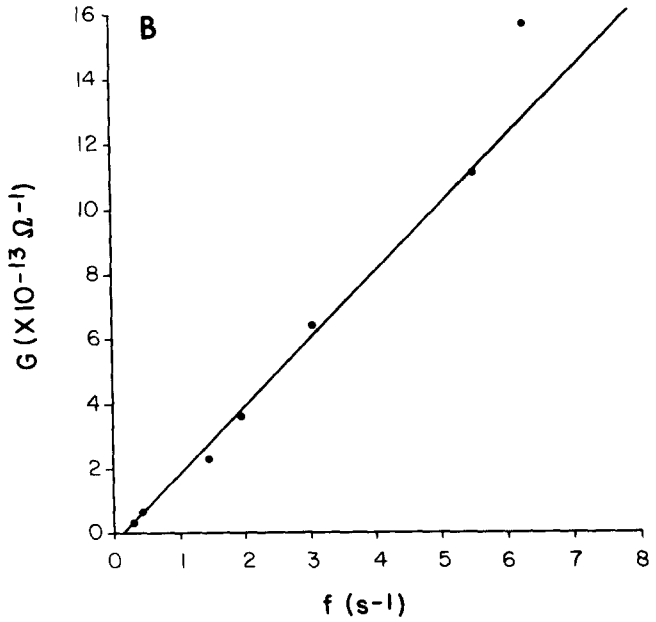

FIGURE 11.

Two points should be made about Fig. 11A. First, the I_s intercept of the least-squares line is, within experimental error, equal to the leakage current at 120 mV. Second, the slope of the line should equal ($q_{av} = i(V) \cdot \tau$), which crosses the membrane per channel. We find $q_{av} = 6.24 \times 10^{-14}$ C/channel. The peak-4 channel current at 140 mV (the middle of the range $120 \leq V \leq 160$ mV; see Fig. 8) is $i = 6.4 \times 10^{-13}$ A. On this basis, we estimate the average channel duration to be 97.5 ms, a factor of ~2.2 greater than our direct measurement of 45 ms.

The most likely origin of this discrepancy is our failure to correct for leakage current (I_l) through the unmodified membrane. We can estimate I_l from the fast channel by measuring the membrane current when no channels are open. This was done by sampling a 60-s run at 2-s intervals and then averaging. I_l was subtracted from I_s and the corrected current was then divided by V to yield the channel-associated conductance (G). All values of G at a given V were averaged and plotted against the averaged channel frequency at that V; the points are plotted in Fig. 11B.

The line in Fig. 11B is fitted to all of the data points except the $V = 160$ mV point, the one at highest G and frequency. We took this liberty because of the difficulty in measuring the channel frequency at high activity; very likely the value of 6.23 channels per second is an underestimate. Taking $g = 4.1 \times 10^{-12}\ \Omega^{-1}$ at $V = 140$ mV (Fig. 8) allows us to calculate the average channel lifetime from the slope of the line in Fig. 11B.[2] The slope is 2.1 ×

[2] In measuring f, we simply counted all channel openings, regardless of whether they occurred from the baseline or during the existence of one or more already open channels. Because G is the time-averaged monazomycin-induced conductance, the slope of the line contains an estimate of τ, the average channel lifetime. This estimate is not biased by the overlap of channels in time.

10^{-13} Ω^{-1} s/channel and the average lifetime is 48.8 ms. (If the least-squares line is drawn to include all of the points, the average life time is found to be ~58 ms.) Thus, this method and the direct one are in reasonable agreement.

Results with Phosphatidylethanolamine Membranes

The properties of single monazomycin channels in phosphatidylethanolamine (PE) membranes (no cholesterol was in the membrane-forming solution) are virtually identical to those already described for phosphatidylglycerol plus cholesterol films. In the first place, inspection of records reveals the existence of compound (or Δ) channels. The mean channel duration is again ~40 ms, independent of membrane potential, and the lifetimes are exponentially distributed. We find that the current-voltage characteristic is well described by Eq. 1 with $B = 0.35$ and $g_o = 3.5 \times 10^{-12}$ Ω^{-1} in 3.6 M KCl. (We actually used 4.0 M KCl, for reasons which later became unclear.) The lower unitary conductance in PE films is presumably a result of the lower surface concentration of univalent cation. (The much lower surface charge density of PE membranes was not completely compensated for by a 36-fold increase in salt concentration.) Finally, channel frequency can vary over a wide range when V is changed, in keeping with our PG results.

DISCUSSION

We will take it for granted that the conductance events (peaks 4 and 5 and the Δ channels) described here represent activity induced by monazomycin molecules and not by some "contaminant" and that these events are the molecular basis for the behavior of the macroscopic conductance. Support for the contention is found in Fig. 11 of this paper and more is provided in the accompanying article (Muller and Andersen, 1982).

The complexity of the individual monazomycin channels seems to fall between the very simple conductance events caused by gramicidin A (Finkelstein and Andersen, 1981) and the multilevel ones seen in alamethecin-doped bilayers (Latorre and Alvarez, 1981). It seems reasonable to say that the resemblance to the gramicidin A events is closer, given that the monazomycin molecules have just two conductance states (which differ by only 25–30%) and that most channels appear to get into only one of the conductance states. This functional similarity obtains despite the presumed structural similarity between monazomycin and alamethecin channels; both seem to be cylinders composed of linear monomers that are arranged as staves of a barrel (see Latorre and Alvarez, 1981), whereas gramicidin A channels are head-to-head dimers of hollow helical monomers.

The form of the individual monazomycin conductance events at first glance seems to imply that the channels have three states, including (at least) one closed state. This, we feel, is an error in terminology that stems from neglecting the fact that the monazomycin channel is not a single molecule. If the picture of a channel as composed of several (approximately six) monomers is correct (Muller and Finkelstein, 1972*a*; Muller and Peskin, 1981), then the independence of channel openings implies that a channel that ceases to conduct also

ceases to exist as a unique, identifiable entity. It is thus most appropriate to designate monazomycin channels as two-state channels. The labile, oligomeric channels induced by certain other membrane modifiers (e.g., gramicidin A, alamethicin, and amphotericin B) should likewise not be thought of as having closed states unless their existence is unambiguously demonstrated. In a similar sense, one may question whether in all cases it is fruitful to assume that chemically or voltage-gated channels in excitable membranes have a fixed molecular identity and therefore have closed states.

A noteworthy property of the monazomycin channels is their very low conductance; this raises a mechanistic question. We note that the extrapolated small-signal conductance for peak-4 channels ($4.1 \times 10^{-12}\ \Omega^{-1}$) is measured with a nominal sodium concentration of ~10 M at the channel entrances. (The cation selectivity of monazomycin channels is intrinsic to the channel and not merely the result of using PG films with their high negative surface charge density [Muller and Finkelstein, 1972*a*].) The channels are thus quite poorly permeant to small univalent cations despite a measurable permeability to cations as large as tetraethylammonium (Heyer et al., 1976). The low conductance and large apparent diameter of the channels can in principle be reconciled if we recall that monazomycin is itself a univalent cation in the pH range we use (Mitscher et al., 1967; Nakayama et al., 1981). These positive charges may thus produce a substantial energy barrier to permeant cations in series with a cation-selective lumen, thereby raising the resistance of the whole path. This is not, however, a unique interpretation of the permeability data, especially since the structure of monazomycin (Nakayama et al., 1981) is such as to allow the positive charges to be quite far from the luminal opening. Electrostatic calculations (Parsegian, 1969; Levitt, 1978) show that the "image force" barrier for transferring a monovalent ion from a bulk aqueous phase into a narrow aqueous channel spanning a bilayer is so great that it would be impossible to see current jumps unless some other factor(s) is available to reduce the free energy of the ion. The likely basis for the reduction of free energy is solvation of the ion by polar groups lining the wall of the channel. A low conductance could thus be compatible with a rather large lumen if a short segment of the channel had a low density of polar groups[3] or if the selectivity of the segment were anionic.

[3] The structure of monazomycin has been solved (Nakayama et al., 1981). The structure is indeed similar to that of the polyene antibiotics, as previously surmised (Muller and Finkelstein, 1972*a*; Heyer et al., 1976; Muller and Peskin, 1981), and is compatible with the barrel-stave model. Most of the polar groups that would line the lumen are hydroxyls and there is indeed a gap that appears less polar. An additional point worth making concerns the instantaneously ohmic behavior of the macroscopic conductance in the range $-100 < V < 100$ mV (Muller and Finkelstein, 1972*a*). If the positive charges were near enough to the channel opening at the trans interface to influence the conductance of a channel, the unitary i-V characteristic would be expected to be nonlinear near $V = 0$, due to the lower cation concentration at the *trans* opening. Because rectifying macroscopic I-V curves can be seen in asymmetrically charged bilayers (R. U. Muller, unpublished observations), it seems less likely that the low value of g is directly caused by the monozomycin amino group.

Supported by National Institutes of Health grant GM 21342, a New York Heart Association Senior Investigator Award, and an Irma T. Hirshl Career-Scientist Award to O. S. A. Some computations were done on equipment supported by NINCDS grant 10987.

Received for publication 3 December 1981 and in revised form 3 June 1982.

REFERENCES

ANDERSEN, O. S., and M. FUCHS. 1975. Potential energy barriers to ion transport within lipid bilayers: studies with tetraphenylborate. *Biophys. J.* **15**:795–830.

BAMBERG, E., and K. JANKO. 1976. Single channel conductance at lipid bilayer membranes in presence of monazomycin. *Biochim. Biophys. Acta.* **426**:447–450.

COX, D. R., and P. A. W. LEWIS. 1966. The Statistical Analysis of Series of Events. Methuen, London.

EHRENSTEIN, G., H. LECAR, and R. NOSSAI. 1970. The nature of the negative resistance in bimolecular lipid membranes containing excitability-inducing material. *J. Gen. Physiol.* **55**:119–133.

EISENMAN, E., J. SANDBLOM, and E. NEHER. 1977. Ionic selectivity, saturation, binding, and block in the grainicidin A channel: preliminary report. *In* Metal-Ligand Interactions in Organic Chemistry and Biochemistry. B. Pullman and N. Goldblum, editors. D. Reidel, Dordrecht-Holland. 1–36.

FINKELSTEIN, A., and O. S. ANDERSEN. 1981. The gramicidin A channel: a review of its permeability characteristics with special reference to the single-file aspect of transport. *J. Membr. Biol.* **59**:155–171.

HEYER, E. J., R. U. MULLER, and A. FINKELSTEIN. 1976. Inactivation of monazomycin-induced voltage-dependent conductance in thin lipid membranes. II. Inactivation produced by monazomycin transport through the membrane. *J. Gen. Physiol.* **67**:731–748.

KOLB, H.-A. 1979. Conductance noise of monazomycin-doped bilayer membranes. *J. Membr. Biol.* **45**:277–292.

LATORRE, R., and O. ALVAREZ. 1981. Voltage-dependent channels in planar lipid bilayer membranes. *Physiol. Rev.* **61**:77–150.

LEVITT, D. G. 1978. Electrostatic calculations for an ion channel. I. Energy and potential profiles and interactions between ions. *Biophys. J.* **22**:209–219.

MITSCHER, L. A., A. J. SHAY, and N. BONONOS. 1967. LL-A491, a new monazomycin-like antibiotic. *Appl. Microbiol.* **15**:1002–1005.

MOORE, L. E., and E. NEHER. 1976. Fluctuation and relaxation analysis of monazomycin-induced conductance in black lipid membranes. *J. Membr. Biol.* **27**:347–362.

MUELLER, P., D. O. RUDIN, H. T. TIEN, and W. C. WESCOTT. 1963. Methods for the formation of single bimolecular lipid membranes in aqueous solution. *J. Phys. Chem.* **67**:534–535.

MULLER, R. U., and O. S. ANDERSEN. 1975. Single monazomycin channels. 5th International Biophysics Congress. U. Lassen and J. O. Wieth, editors. Abstract 367.

MULLER, R. U., and O. S. ANDERSEN. 1982. Monazomycin-induced single channels. Initiation of single-channel activity, and the molecular basis for the voltage-dependence. *J. Gen. Physiol.* **80**:427–449.

MULLER, R. U., and A. FINKELSTEIN. 1972*a*. Voltage-dependent conductance induced in thin lipid membranes by monazomycin. *J. Gen. Physiol.* **60**:263–284.

MULLER, R. U., and A. FINKELSTEIN. 1972*b*. The effects of surface charge on the voltage-

dependent conductance induced in thin lipid membranes by monazomycin. *J. Gen. Physiol.* **60:**285–306.

MULLER, R. U., G. ORIN, and C. S. PESKIN. 1981. The kinetics of monazomycin-induced voltage-dependent conductance. I. Proof of the validity of an empirical rate equation. *J. Gen. Physiol.* **78:**171–200.

MULLER, R. U., and C. S. PESKIN. 1981. The kinetics of monazomycin-induced voltage-dependent conductance. II. Theory and a demonstration of a form of memory. *J. Gen. Physiol.* **78:**201–229.

NAKAYAMA, H., K. FURIHATA, H. SETO, and N. ŌTAKE. 1981. Structure of monazomycin, a new ionophorous antibiotic. *Tetrahedron Lett.* **22:**5217–5220.

NEHER, E., and B. SAKMANN. 1976. Single-channel currents recorded from membrane of denervated frog muscle fibers. *Nature (Lond.).* **260:**779–802.

PARSEGIAN, A. 1969. Energy of an ion crossing a low dielectric membrane: solutions to four relevant electrostatic problems. *Nature (Lond.).* **221:**844–846.

SZABO, G., G. EISENMAN, and S. CIANI. 1969. The effects of the macrotetralide actin antibiotics on the electrical properties of phospholipid bilayer membranes. *J. Membr. Biol.* **1:**346–382.

WANKE, E., and G. PRESTIPINO. 1976. Monazomycin channel noise. *Biochem. Biophys. Acta.* **436:**721–726.